Injectable Drug Delivery Systems of Active Ingredient Revisited: *In Vitro-In Vivo* Relationships Using Human Clinical Data

Harshvardhan Modh, Daniel Juncheng Fang, Yi Hsuan Ou, Jia Ning Nicolette Yau, Tatyana Kovshova, Shakti Nagpal, Julian Knoll, Chantal M. Wallenwein, Kuntal Maiti, Subdhas Bhowmick, Svetlana Gelperina, Giorgia Pastorin, Matthias G. Wacker

PII: S0378-5173(21)00879-6
DOI: https://doi.org/10.1016/j.ijpharm.2021.121073
Reference: IJP 121073

To appear in: *International Journal of Pharmaceutics*

Received Date: 25 April 2021
Revised Date: 30 August 2021
Accepted Date: 31 August 2021

Please cite this article as: H. Modh, D. Juncheng Fang, Y. Hsuan Ou, J. Ning Nicolette Yau, T. Kovshova, S. Nagpal, J. Knoll, C.M. Wallenwein, K. Maiti, S. Bhowmick, S. Gelperina, G. Pastorin, M.G. Wacker, Injectable Drug Delivery Systems of Active Ingredient Revisited: *In Vitro-In Vivo* Relationships Using Human Clinical Data, *International Journal of Pharmaceutics* (2021), doi: https://doi.org/10.1016/j.ijpharm.2021.121073

Injectable Drug Delivery Systems of Active Ingredient Revisited: *In Vitro-In Vivo* Relationships Using Human Clinical Data

Harshvardhan Modh[1], Daniel Juncheng Fang[1], Yi Hsuan Ou[1], Jia Ning Nicolette Yau[1], Tatyana Kovshova[2,3], Shakti Nagpal[1], Julian Knoll[4], Chantal M. Wallenwein[4,5], Kuntal Maiti[6], Subdhas Bhowmick[6], Svetlana Gelperina[3], Giorgia Pastorin[1], Matthias G. Wacker[1]*

1 National University of Singapore, Faculty of Science, Department of Pharmacy, Singapore.
2 Lomonosov Moscow State University, Leninskiye Gory 1, 119991, Moscow, Russia.
3 D. Mendeleev University of Chemical Technology of Russia, Miusskaya pl. 9, 125047, Moscow, Russia.
4 Goethe University, Institute of Pharmaceutical Technology, Germany.
5 Fraunhofer-Institute for Translational Medicine and Pharmacology, Department of Pharmaceutical Technology, Germany.
5 Sun Pharmaceutical Industries Ltd., Vadodara, India.

*Corresponding author:
Associate Professor Matthias G. Wacker
Department of Pharmacy │ Faculty of Science
National University of Singapore
6 Science Drive 2
Singapore 117545
phamgw@nus.edu.sg
Phone +65 6516 1133
Fax +65 6779 1554
pharmacy.nus.edu.sg

Abstract

A growing number of nanomedicines entered the clinical trials and improved our understanding of the *in vivo* responses expected in humans. The *in-vitro* drug release represents an important critical quality attribute involved in pharmacokinetics. Establishing *in vitro-in vivo* relationships for nanomedicines requires a careful analysis of the clinical data with respect to the unique differences between drugs and nanomedicines. Also, the biorelevant assay must reflect the release mechanism of the carrier. Four drug delivery systems of Active Ingredient were evaluated for their *in vitro* release behavior under biorelevant conditions using the dispersion releaser. The pharmacokinetics observed during the first-in-men clinical trials were analyzed using a custom-made physiologically-based nanocarrier biopharmaceutics model. The drug product Lipodox® and the clinical candidate NanoCore-7.4 were evaluated to validate the model. Afterward, the *in vivo* performance of the preclinical candidates NanoCore-6.4 and Active Ingredient-loaded nano-cellular vesicle technology systems (nCVTs-Dox) were predicted. *In vitro* and *in vivo* release were in good correlation as indicated by the coefficients of determination of 0.98648 (NanoCore-7.4) and 0.94107 (Lipodox®). The predictions required an estimation of the carrier half-life in blood circulation leading to considerable uncertainty. Still, the simulations narrow down the possible scenarios in the clinical evaluation of nanomedicines and provide a valuable addition to animal studies.

Graphical Abstract

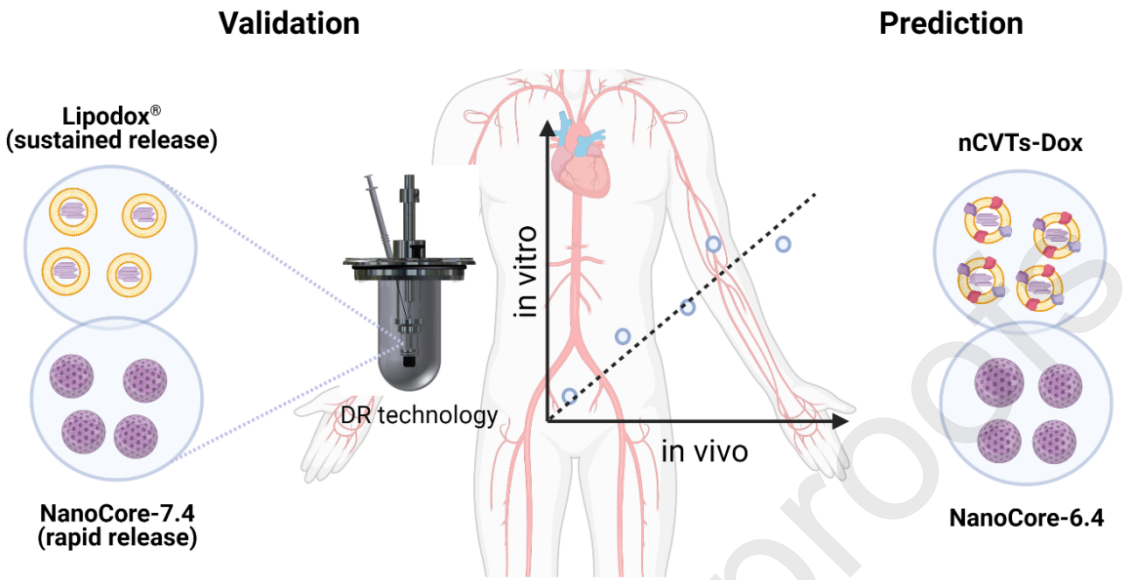

Abbreviations

CE	Cellulose Ester
DLS	Dynamic Light Scattering
DR	Dispersion Releaser
EPR	Enhanced Permeability and Retention
FBS	Fetal Bovine Serum
HPLC	high performance liquid chromatography
IVIVC	*in vitro-in vivo* correlation
IVIVR	*in vitro-in vivo* relationship
LOD	Limit of detection
LOQ	Limit of quantification
nCVTs-Dox	Active Ingredient-loaded nano-cellular vesicle technology systems
MWCO	Molecular Weight Cut-off
NTA	Nanoparticle Tracking Analysis
PBBM	Physiologically Based Biopharmaceutics Model
PBNB model	Physiologically Based Nanocarrier Biopharmaceutics model
PBS	Phosphate buffered saline
PLGA	Poly lactide-co-glycolide
PPSA	Partial Parameter Sensitivity Analysis
PVA	Poly(vinyl alcohol)
rpm	revolutions per minute
SD	Standard Deviation
STELLA	Systems Thinking, Experimental Learning Laboratory with Animation
USP	United States Pharmacopeia

1. Introduction

An *in vitro–in vivo* correlation (IVIVC) is defined as a predictive mathematical model, describing the relationship between the *in vitro* features of a drug delivery system and relevant *in vivo* responses such as the plasma concentration-time profile. IVIVC plays a key role in the development of new drug products and serves as a link between the material attributes of drug carriers and clinical performance (Shen and Burgess, 2015). In the area of peroral dosage forms, they provide evidence for the application of *in vitro* drug release testing as a surrogate for *in vivo* bioavailability (Cheng et al., 2014). For some correlations, further model assumptions are required to explain the interplay between formulation properties and the plasma concentration (Mast et al., 2021). They are sometimes called *in vitro-in vivo* relationships (IVIVRs) (Mast et al., 2021).

In the area of nanomedicines, even after more than 30 years of clinical research, establishing this mathematical relationship has been a major challenge. One of the reasons is the limited availability of suitable *in vitro* methods that enable a quantitative assessment of the drug release under biopredictive conditions (Fecioru et al., 2019; Nothnagel and Wacker, 2018). The dispersion releaser (DR) technology can separate the free and the colloidal fraction of the drug in the presence of serum proteins and plasma (Janas et al., 2017; Wallenwein et al., 2019). It renders selectivity and sensitivity of the method and separates particle populations from the release medium at an acceptable rate (Jablonka et al., 2020a; Jablonka et al., 2019; Janas et al., 2017; Nothnagel and Wacker, 2018). Based on the release rates obtained *in vitro,* a retrodiction of the *in vivo* pharmacokinetics of the injectable drug product Foscan® was achieved (Jablonka et al., 2019). In a second step, the performance of the investigational drug product Foslip® was predicted (Jablonka et al., 2020a).

Another important challenge in the development of the IVIVC lies in the complexity of plasma pharmacokinetics following the intravenous administration of the drug delivery system. Once injected into a vascular system, the drug release from the carrier is solely responsible for the availability of the free drug in blood circulation (Kovshova et al., 2021; Nagpal et al., 2020). Therefore, the plasma extraction method represents an important error source in the evaluation of bioavailability. Consequently, the procedures and standards defined for extravascular

administration of medicines cannot be extrapolated to nanomedicines. Some of the most important differences are presented in Table 1.

Table 1: Differences between the peroral/extravascular administration of drugs and nanomedicines obtained from different literature sources (El-Kareh and Secomb, 2000; Hinderliter and Saghir, 2014; Mast et al., 2021; Ritschel and Kearns, 2009).

Extravascular / Peroral administration	Nanomedicine
Absorption overlaps with the release (liberation) phase.	Infusion of the carrier overlaps with the release phase.
Drug release at the administration site is followed by the absorption of the drug.	Drug release in the blood plasma is followed by the distribution of the released drug.
The drug in the blood plasma is in the monomolecular form.	The drug in the blood plasma is encapsulated or in monomolecular form.
Bioavailability is driven by drug release and absorption.	Bioavailability is driven by the drug release.
Elimination is dominated by the behavior of the compound and its metabolites.	The carrier-bound and the free fraction of the drug are accumulated and eliminated independently.
Bioavailability (defined as the amount of the drug appearing in the blood plasma) is 100% when the drug is absorbed completely.	Bioavailability (defined as the amount of the drug appearing in the blood plasma) is 100% when the drug is released completely.
Drug absorbed into systematic circulation is responsible for the pharmacological and toxicological effects.	Drug released in the blood plasma and the accumulated fraction together are responsible for the pharmacological and toxicological effects.

After the infusion of the carrier into blood circulation, the carrier-bound fraction of the drug circulates in the vascular system and changes the biodistribution and elimination behavior of the compound (Kovshova et al., 2021; Nagpal et al., 2020). The accumulation and targeting of the drug often lead to a local increase in the drug concentration. Although both steps, the release of the drug in blood circulation and the accumulation of the carrier are pharmacologically and toxicologically relevant absorption steps, only the released fraction is monitored during the phase I clinical trials and can be used to establish the IVIVC (Mast et al., 2021). In addition, the total plasma concentration-time profile represents a convoluted signal, combining the free and the carrier-bound fraction (Jablonka et al., 2020a; Jablonka et al., 2019). Hence establishing the IVIVC requires deterministic elements rather than a stochastic approach (Nagpal et al., 2020).

Today, Active Ingredient is one of the most potent antineoplastic drugs and was applied for the treatment of a wide variety of solid tumors such as ovarian cancer or glioblastoma multiforme (Bhowmik et al., 2018; Filon et al., 2017). The cardiotoxicity of the compound led to the development of a significant number of nanomedicines such as the long-circulating liposomal

formulation Active Ingredient® and its generic counterpart Active Ingredient Hydrochloride liposome injection of Sun Pharma (known as Lipodox® in India) (Alibolandi et al., 2017). Additionally, a considerable number of nanoparticle formulations including the fast-releasing clinical formulation prototypes NanoCore-7.4 and NanoCore-6.4 were developed (Kovshova et al., 2021; Maksimenko et al., 2019). For this purpose, Active Ingredient was encapsulated into a porous matrix of polylactide-co-glycolide (PLGA), leading to a very rapid drug release (Maksimenko et al., 2019; Pereverzeva et al., 2019; Zhang et al., 2020). The latest generation of drug delivery systems utilizes Active Ingredient-loaded nano-cellular vesicle technology systems (nCVTs-Dox) (Goh et al., 2018). Here, cellular proteins embedded into the liposomal membrane increase tumor uptake and lead to an accumulation comparable to the pegylated liposomes in mice (Goh et al., 2018; Yong et al., 2020).

The present study emphasizes the development of biopredictive *in vitro* release methods based on the DR technology. The corresponding *in vivo* release was identified using the physiologically-based nanocarrier biopharmaceutics (PBNB) model (Kovshova et al., 2021; Nagpal et al., 2020). After defining the model structure using the programming language Systems Thinking, Experimental Learning Laboratory with Animation (STELLA) and selection of parameter ranges, a model-based deconvolution of the total plasma concentration-time profile was carried out by differential evolution. The IVIVC for Lipodox® and NanoCore-7.4 was used to validate the biopredictive assay. As a next step, we simulated the pharmacokinetic behavior of the two novel formulation candidates nCVTs-Dox and NanoCore-6.4.

2. Materials and methods

2.1. Materials and chemicals

Active Ingredient hydrochloride (98%) was purchased from Cayman Chemical (Michigan, USA). Adriamycin was obtained from the National University Hospital Pharmacy (Singapore). The generic drug formulation Lipodox® was kindly provided by Sun Pharmaceutical Industries Ltd (Mumbai, India). PLGA for the synthesis of NanoCore-6.4 and NanoCore-7.4 was kindly provided by Corbion. Fetal Bovine Serum (FBS) was purchased from Biowest (Nuaillé, France). Active Ingredient-Active Ingredient (Pen-Strep) solution was purchased from Life Technologies Corporation (Carlsbad, Canada). The DR devices were kindly provided by Pharma Test Apparatebau AG (Hainburg, Germany). More information on the specifications of the instrument (patent no. WO2015039749A1) has been published previously (Janas et al., 2017; Villa Nova et al., 2015; Wallenwein et al., 2019). A cellulose ester (CE) dialysis membrane Spectra/Por® Biotech CE Tubing with a molecular weight cut-off (MWCO) of 50 and 300 kDa with a flat width of 31 mm and a diameter of 20 mm was purchased from VWR International GmbH (Darmstadt, Germany). All other chemicals were of analytical or high-performance liquid chromatography (HPLC) grade and used as received.

2.2. Synthesis of NanoCore-7.4 and NanoCore-6.4

The clinical formulation prototype NanoCore-7.4 was manufactured as reported previously (Maksimenko et al., 2019). Briefly, Active Ingredient-loaded PLGA nanoparticles were synthesized by using the double emulsion solvent evaporation technique (w/o/w). An amount of 120 mg of Active Ingredient hydrochloride was dissolved in 4.8 mL of hydrochloric acid (0.001 N) and added to a solution of 1.2 g of PLGA in 7.2 mL of dichloromethane. The mixture was emulsified using an Ultra-Turrax T18 Basic high shear rotor-stator mixer (IKA Industrie- und Kraftfahrzeugausrüstung GmbH, Königswinter, Germany) for 1 min at 23,600 revolutions per minute (rpm). The pre-emulsions were added to a volume of 60 mL of an aqueous solution of Poly(vinyl alcohol) (PVA) (1%) in phosphate-buffered saline (PBS) at pH 7.4 (to obtain NanoCore-7.4) or pH 6.4-6.5 (to obtain NanoCore-6.4). The mixture was further emulsified using the high shear rotor-stator mixer (Ultra-Turrax T-18) over 2 min. To further reduce the particle size, the emulsion was passed through a high-pressure homogenizer (Microfluidizer M-110P, Microfluidics, Newton, USA) at 15,000 psi for 3 min while maintaining a temperature of

+20 °C. The remaining organic solvent was removed under vacuum (20 mbar) using a rotary evaporator (Laborota 4000, Heidolph Instruments GmbH and Co. KG, Schwabach, Germany). The suspension was passed through a glass porous filter (pore size 90-150 µm). A total amount of 5% (w/v) of Active Ingredient was added as a cryoprotectant. The dispersions were filled into freeze-drying vials (1.5 mL per vial) and freeze-dried using an Alpha 2-4 LSCplus freeze dryer (Martin Christ GmbH, Osterrode, Germany). To modify the surface of the nanoparticles, the freeze-dried nanoparticles were resuspended in an aqueous solution of poloxamer 188 (1%) and incubated for 30 min before further characterization (Kovshova et al., 2021).

2.3. Synthesis of nano-cell vesicle technology systems

An amount of 2 mg of 1,2-dioleoyl-sn-glycero-3-phosphocholine (DOPC) and cholesterol (7:3 mol %) was dissolved in chloroform and a thin film was formed using rotary evaporation. To prepare Active Ingredient-loaded nCVTs (nCVTs-Dox), cell ghosts (obtained from 1 x 10^7 cells) were manufactured as described previously (Goh et al., 2018) and resuspended in 250 mM ammonium phosphate buffer and extruded through a 5 µm polycarbonate membrane. The extruded dispersion was then used to rehydrate the lipid film. Afterward, the mixture was subsequently sonicated for at least 30 minutes, before further extrusion was performed in a jacketed extruder (Genizer™, Los Angeles, USA) at 35 °C through a series of filters with pore sizes of 0.4 µm, 0.2 µm, and 0.1 µm. The buffer of the final nCVTs-Dox dispersion was changed to PBS, before the addition of Active Ingredient (200 $\mu g \cdot ml^{-1}$) in a ratio of 1:1 (v/v). The remote loading procedure was conducted at 37 °C for 1 hour. The un-encapsulated Active Ingredient was removed using a Sephadex G50 column (Ge Healthcare, USA) after pre-equilibration with PBS.

2.4. Determination of particle size, size distribution, and zeta potential

The particle size, size distribution, and zeta potential of NanoCore-6.4, NanoCore-7.4, Lipodox®, and nCVTs-Dox were investigated by means of dynamic light scattering (DLS) using a Litesizer™ 500 (Anton Paar GmbH, Graz, Austria) equipped with 658 nm single-frequency laser diode, providing 40 mW. Each measurement was performed in PBS at 25°C at a detection angle of 175° in a single-use cuvette. The zeta potential was measured by electrophoretic light scattering using the same system equipped with omega cuvettes. All experiments were performed in triplicate.

Additionally, nanoparticle tracking analysis (NTA) was carried out to measure the particle size and size distribution of all formulations in the release medium (PBS 7.4, 10% FBS). A Nanosight NS300 (Malvern Instruments, Malvern, UK), equipped with a 532 nm laser was used. During the measurement, the chamber was kept at a constant temperature of 25 °C. The software used for capturing and analyzing the data was NTA 3.2 (Dev Build 3.2.16, Malvern, UK). Three captures, each lasting 60 seconds, were analyzed per sample, resulting in a detection of at least 2000 valid particle tracks per sample. The particle diameters were calculated using the Stokes-Einstein equation. The size was compared to the reference measurements.

2.5. Quantification of Active Ingredient using high-performance liquid chromatography

The HPLC system (Chromaster, VWR Hitachi, Tokyo, Japan) was composed of a fluorescence detector (5440), a pump (5160), an autosampler (5260), and a column oven (5310). A PerfectSil reversed-phase column (150 x 4.6 mm, pore size 110 Å, particle size 5 µm) and a pre-column of the same material were used as stationary phase (Phenomenex Ltd., Aschaffenburg, Germany). During the run, the column was kept at a constant temperature of 35 °C. The mobile phase consisted of acetonitrile and an aqueous solution of 0.1% trifluoroacetic acid (32:68 (v/v)). The flow rate was set to 1 mL/min. The drug was detected using excitation and emission wavelengths of 470 nm and 555 nm, respectively. Linearity was observed over a concentration range of 5-1000 $ng \cdot mL^{-1}$. The limit of detection (LOD) and limit of quantification (LOQ) were determined to be 54.8 ng/mL and 166.1 ng/mL, respectively. All samples were diluted with the mobile phase before the injection. All experiments were performed in triplicate.

2.6. Membrane permeation and drug stability

The membrane permeation and drug stability studies were performed in the stainless steel version of the DR (Pharma Test Apparatebau AG, Hainburg, Germany) (Jablonka et al., 2019; Janas et al., 2017; Villa Nova et al., 2015; Wallenwein et al., 2019) under conditions comparable to the *in vitro* release experiment (see section 2.7). A USP dissolution apparatus 2 (Pharma Test Apparatebau AG, Hainburg, Germany) equipped with a mini-vessel configuration was used (Janas et al., 2017). The DR comprises a small cage in the center of the dissolution vessel representing the donor chamber. A mini-vessel represented the acceptor compartment. A CE dialysis membrane with an MWCO of 300 kDa was prepared according to the instructions of the manufacturer and mounted around the donor compartment. A release medium supplemented with 10% (v/v) of FBS and 1% (v/v) of Pen-Strep solution was employed. The

temperature was kept constant in the range of 37 °C ± 0.5 °C and the stirring speed was set to 50 revolutions per minute (rpm).

To determine the degradation rate of Active Ingredient, a total amount of 206 µg of Active Ingredient was added to the acceptor compartment. A volume of 160 mL of release medium was used. The drug was quantified from the acceptor compartment at 1, 3, 6, 24, and 48 h. To measure the membrane permeation rate, the same amount of Active Ingredient was dissolved in 3 mL of release medium and added to the donor compartment. A total volume of 157 mL of release medium was used as acceptor medium. The concentration of Active Ingredient in the acceptor compartment was measured at pre-defined time points for 48 h. After sample collection, an equal volume of fresh release medium was added to the acceptor compartment.

2.7. *In vitro* release experiments using the dispersion releaser technology

An amount of the freeze-dried NanoCore-7.4 particles and nCVTs-Dox corresponding to 205.18 µg of Active Ingredient was dispersed in the release media by gentle mixing and added to the donor compartment. For Lipodox®, a volume corresponding to 164.14 µg was added to the donor compartment. Under these conditions, the initial dilution of Active Ingredient-loaded formulations in the DR corresponds to the dilution expected for the estimated blood plasma volume of each patient population (2.756 L for Lipodox® and 1.928 L for NanoCore-7.4). This information was obtained by pharmacokinetic analysis of the clinical data published by Bhowmick *et al*. (50 mg/m², 41 patients) (Bhowmik et al., 2018) and Filon *et al*. (48 mg/m², 21 patients) (Filon et al., 2017). For nCVTs-Dox, a blood plasma volume similar to the one observed for NanoCore-7.4 was assumed. The volumes of donor and acceptor compartments were 3 mL and 157 mL, respectively. The release medium supplemented with 10% (v/v) of FBS and 1% (v/v) of Pen-Strep solution was employed.

The *in vitro* release experiments were conducted over 6 h. A sample volume of 600 µL was collected at each time point (5, 10, 15, 20, 30, 45, 60, 75, 90, 105 min, 2, 3, 4, 5, and 6 h). After the collection of each sample, a similar volume of fresh release medium was added to the acceptor compartment.

2.8. Calculation of the degradation-corrected drug release profile

In presence of serum, Active Ingredient rapidly degrades into several metabolites. Therefore, a mathematical model was applied to calculate the degradation-corrected release profiles. This recovery model is described in more detail in the **supplementary materials (S1)**. To study the degradation in the DR, Active Ingredient was added to the acceptor compartment and the changes in the drug concentration were monitored over time. The degradation rate was obtained by fitting the degradation curve, followed by a profile correction using a recovery model in STELLA.

2.9. Normalization of drug release profiles

The degradation rate of the drug (k_{deg}) and the membrane permeation rate (k_m) was used for the normalization of the release profile. To quantify the membrane permeation rate constant (k_M), an aqueous solution of Active Ingredient was dialyzed in a reference experiment (Janas et al., 2017; Xie et al., 2015). The differential equations used for the calculation of the drug concentration-time profile are provided in more detail in the **supplementary materials S1-S3**. More information on the *four-step* model has been published previously (Jablonka et al., 2019; Jablonka et al., 2020b; Janas et al., 2017; Wallenwein et al., 2019; Xie et al., 2015). The model was written and executed in STELLA.

2.10. Establishing the *in vitro-in vivo* Correlation

The IVIVC was established based on the *in vivo* release obtained by pharmacokinetic analysis of the total plasma concentration using the PBNB model (Kovshova et al., 2021; Nagpal et al., 2020). An illustration of the model structure is presented in Figure 1.

In brief, the PBNB model utilizes a model-based deconvolution of the total plasma concentration-time curve of the nanocarrier using the pharmacokinetic parameters of the free drug (V_{DF}, k_{12}, k_{21}, k_e) and the estimated blood plasma volume of the patient population. This parameter is assumed to correspond to the volume of distribution of the carrier-bound fraction (V_{DC}). Additionally, the infusion rate (k_{inf}) obtained from the clinical protocol of each clinical trial and the initial distribution phase (k_{trans}) observed for pegylated liposomes (approximately 15 min) have been identified to account for a delay in the influx of the drug formulation into the blood plasma. The volumes of distribution of the encapsulated fraction (V_{DC}) and the free drug (V_{DF}) are responsible for the relative influence of the pharmacokinetic parameters of each

fraction (the free and the carrier-bound fraction) on the total plasma concentration, which results in a different simulated *in vivo* release. The pharmacokinetic parameters used for these calculations are summarized in Table 2. The half-life ($t_{1/2}$) represents the half-life of the carrier-bound drug (simulated nanocarrier fraction).

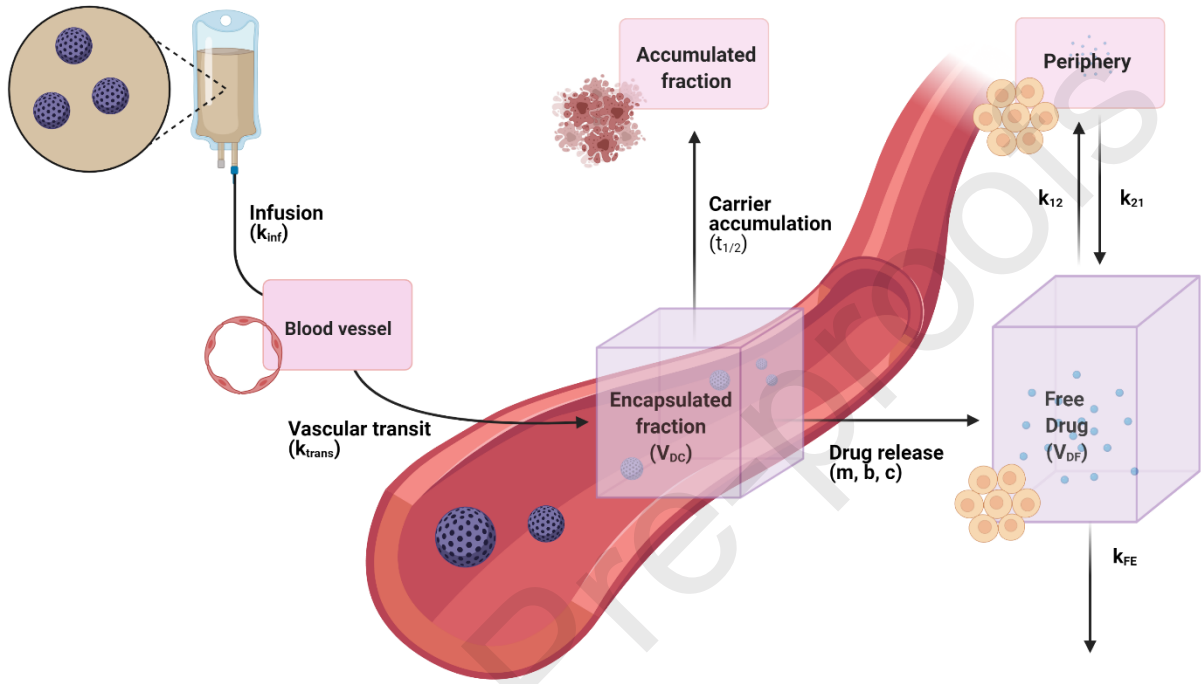

Figure 1. Illustration of the PBNB model used for *in silico* analysis and IVIVC development. After a short period of vascular transit represented by the transport rate (k_{trans}) the carrier enters the vascular system with a volume of distribution (V_{DC}). This is followed by the processes of drug release (m,b,c) and carrier accumulation ($t_{1/2}$). Once the drug has been released it follows a conventional two-compartment model with a volume of distribution (V_{DF}), distribution into the periphery (k_{12}, k_{21}) and elimination (k_{FE})

The *in vivo* drug release rate was calculated using the three-parametric reciprocal powered time (3RPT) model. It utilizes the three release parameters m, b, and c. A more detailed description of 3RPT model was added to the **supplementary materials (S2)**. It accurately describes a wide variety of the release curves without providing more information on the exact mechanism of the release. In the context of pharmacokinetic simulation and modeling, it is applied for the 'unbiased' extraction without giving preference to a specific process (e.g. diffusion, dissolution) (Feczko et al., 2019; Janas et al., 2017; Wallenwein et al., 2019). Another important parameter, calculated by the PBNB model is the targeting capability (F_{target}). It represents the fraction of the dose accumulated in the body in the encapsulated state and is calculated using equation 1 (Nagpal et al., 2020):

$$F_{target} = \frac{m_{accumulated}}{Dose} \quad (1)$$

The parameters used for simulation of the pharmacokinetics of NanoCore-6.4 and nCVTs-Dox were reported previously (Nagpal et al., 2020), as presented in Table 2. The *in vivo* release parameters of Lipodox® and NanoCore-7.4 are the mathematical representation of the *in vitro* release in the PBNB model. After validation of the biorelevant assay (using the IVIVC), pharmacokinetics of the drug formulations NanoCore-6.4 and nCVTs-Dox were estimated based on their *in vitro* release.

Table 2: Pharmacokinetic parameters of the drug carrier and the free drug utilized for the deconvolution of the total plasma concentration-time profile and the simulations performed using the PBNB model. For the simulations of NanoCore-6.4 and nCVTs-Dox half-lives were simulated in multiple ranges based on the formulation characteristics.

Formulation		Lipodox®	NanoCore-7.4	NanoCore-6.4	nCVTs-Dox
$t_{½}$	(h)	89.79	0.712	0.712-89.79 0.57-0.85	0.712-89.79 14.34-23.32 11.47-17.21
$k_{transit}$	(h^{-1})	22.169	52.265	22.169-52.265	22.169-52.265
V_{DC}	(L)	2.756	1.928	1.928	1.928
k_{21}	(h^{-1})	0.478	0.636	0.636	0.636
k_{12}	(h^{-1})	9.376	8.331	8.331	8.331
k_e	(h^{-1})	2.272	1.795	1.795	1.795
V_{DF}	(L)	27.22	26.908	26.908	26.908
In vivo release parameters	b	0.001	0.207	-	-
	m	9.936	7.227	-	-
	c	0.0817	55.758	-	-
In vitro release parameters		Scaled *In vitro* profile			

2.11. Estimating the pharmacokinetics of Active Ingredient-loaded drug formulations

To estimate the pharmacokinetics of NanoCore-6.4 and nCVTs-Dox, the *in vitro* release of the validated biorelevant *in vitro* assay was assumed to be predictive for the *in vivo* release behavior of the drug formulations. This was confirmed by the IVIVC, established for NanoCore-7.4 and Lipodox® (section 2.10). In the area of nanomedicines, the release of the drug from the carrier is solely responsible for the bioavailability of the drug in the blood plasma.

The pharmacokinetic parameters of free Active Ingredient (V_{DF}, k_{12}, k_{21}, k_e) and the volume of distribution of the carrier (V_{DC}) were assumed to reflect the one observed for the patient population treated with NanoCore-7.4 (Filon et al., 2017; Nagpal et al., 2020).

The estimation of V_{DC} is consistent with a retrospective analysis of several clinical data sets and supportive

evidence confirming a localization of nanomedicines in the vascular system (Nagpal et al., 2020). Two of the parameters presented in Table 2 depend on the structure of the drug delivery system and have not been reflected by the *in vitro* assay. The initial distribution phase is represented by the vascular transit rate (k_{trans}), while the accumulation of the carrier in the cellular body of the blood and the peripheral organs is represented by the carrier half-life ($t_{1/2}$) (Nagpal et al., 2020). Both parameters were simulated in a range observed for NanoCore-7.4 and Lipodox®. These parameters are major uncertainties in the simulation and will be discussed in the Results and Discussion section. Both formulations, nCVTs-Dox, and NanoCore-6.4 underwent early preclinical studies. Also, they have been characterized for their physicochemical characteristics. This information has been the basis for the estimation of pharmacokinetics.

With regards to the estimated half-life ($t_{1/2}$), the first simulation covered the validated range of the model assuming that the half-lives of the unknown formulations fall into the wide range covered by NanoCore-7.4 and Lipodox® (0.712 and 89.79 h). In the second simulation, for NanoCore-6.4, a strong similarity to the pharmacokinetic behavior of NanoCore-7.4 was assumed. This is in line with the outcome of the preclinical studies (Kovshova et al., 2021). An expanded probable range of ± 20% relative to the identified half-life (0.712 h) was assumed. For nCVTs, the lipid composition and particle size were compared to the liposomal formulations tested in humans.

The selection of the parameter ranges as well as the outcomes will be presented in the Results and Discussion section. The authors are aware of the uncertainties of this estimation. However, with respect to the current state-of-the-art, there are no *in vitro* or *in vivo* models available to provide a better estimation.

2.12. Software and statistics

The PBNB model was written and executed in STELLA. After analyzing the pharmacokinetic profile of the free drug using Lixoft MonolixSuite 2020 (Antony, France), the initial estimates and parameter ranges were defined in the optimization interface of Stella Architect (v2.0.1, isee systems, Lebanon, USA). This was followed by an automated calculation of the *in vivo* release using the differential evolution algorithm (Storn and Price, 1997). A workflow for the development of the IVIVC is presented in Figure 2.

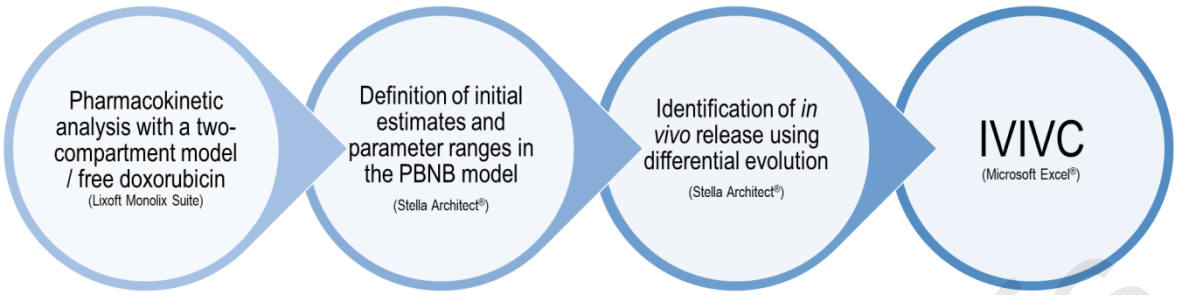

Figure 1. Workflow for the development of the IVIVC beginning with the pharmacokinetic data of the free drug.

The same software was used for the calculation of k_M and the normalization of the release profiles (supplementary materials, S1-3). The IVIVC was established using Microsoft Excel® 365 (Nagpal et al., 2020). All procedures for the extraction and evaluation of the pharmacokinetic profiles using the PBNB model have been published previously. All graphs were created with OriginPro 2019 (OriginLab Corporation, Northampton, USA).

3. Results and discussion

Following the approval of Active Ingredient® in the 1990s, a wide variety of nanomedicines has entered clinical trials. Still, after more than two decades, the relationship between the material properties of non-biological complex drugs and the clinical responses is poorly understood (Shen and Burgess, 2015). Here we establish a direct mathematical relationship between the *in vitro* release quantified with a biorelevant release assay using the DR technology, and the *in vivo* release observed for Active Ingredient-loaded nanomedicines. To verify the assay, two clinically relevant drug formulations Lipodox® and NanoCore-7.4 were tested (Bhowmik et al., 2018; Filon et al., 2017). While Lipodox® is a sustained-release formulation of Active Ingredient, NanoCore-7.4 releases the drug within the first 2 hours after injection. The *in vivo* release rates were extracted using the PBNB model (Kovshova et al., 2021; Nagpal et al., 2020). Importantly, the *in vivo* release from nanomedicines is solely responsible for the bioavailability of the free drug in the blood plasma and is not followed by any further absorption step (Kovshova et al., 2021; Nagpal et al., 2020) (Figure 1). The validated *in vitro* assay was used to estimate human pharmacokinetics of the drug formulations NanoCore-6.4 and nCVTs-Dox. The significant uncertainties but also the potential of this methodology will be discussed in the later sections.

3.1. Physicochemical characteristics of nanomedicines

All drug formulations were characterized with regard to their particle size, size distribution, and zeta potential (Table 3). For Lipodox®, NanoCore-6.4, and NanoCore-7.4, the diameter was within the range reported in the literature (Bhowmik et al., 2018; Kovshova et al., 2021; Maksimenko et al., 2019). For nCVTs-Dox, a particle size of 194 ± 12 nm was found.

Table 3: Physicochemical parameters of the drug formulations evaluated.

Formulation	Particle diameter [nm]	Polydispersity index [%]	Zeta potential [mV]
Lipodox®	86 ± 2	14.5 ± 2.4	-30.8 ± 5.1
NanoCore-7.4	105 ± 12	14.4 ± 1.1	-10.46 ± 1.3
nCVTs-Dox	194 ± 12	20.6 ± 1.0	-14.4 ± 3.68
NanoCore-6.4	137 ± 7	30.1 ± 6.9	-6.40 ± 2.3

The synthesis of the two drug formulations NanoCore-7.4 and NanoCore-6.4 has been described previously (Kovshova et al., 2021; Maksimenko et al., 2019). Only minor differences in the physicochemical characteristics were observed. Considering the polydispersity index

ranging from 14.5-30%, no significant effect on the overall circulation time would be expected. This was confirmed by a pharmacokinetic study in rats (Kovshova et al., 2021).

3.2. Chemical stability and membrane permeation of Active Ingredient

Before the release experiments, chemical stability and permeation of Active Ingredient were measured in the DR. Following the release of Active Ingredient from the carrier into the donor compartment, the free drug permeates through a dialysis membrane before it reaches the acceptor compartment. To account for the kinetics of this membrane transport, the permeability coefficients were determined. The conditions were comparable to the ones selected for the release experiment. A permeation rate constant of $1.72 \cdot 10^{-3} \pm 0.28 \cdot 10^{-3}$ $cm^2 \cdot h^{-1}$ was found. Expectedly, the permeation rate was slightly lower as compared to other compounds (Jablonka et al., 2020b; Janas et al., 2017). Strong interactions between the drug and the membrane are responsible for this effect.

Another parameter of influence is the degradation of Active Ingredient in the biorelevant medium. In presence of serum, the compound rapidly degrades to different metabolites (Laubrock et al., 2000). Therefore, the degradation rate of Active Ingredient was determined at different serum concentrations over 48 h (**supplementary materials, Table S1**). The selected serum concentration of 10% led to moderate degradation. At higher serum concentrations (50%, 75%, and 90%), Active Ingredient was converted to doxorubicinol (the major degradation product of Active Ingredient) more rapidly. This was in line with previous findings in human plasma (Kovshova et al., 2021). The degradation of Active Ingredient has a strong impact on the release behavior by affecting the concentration gradient at the lipid bilayer. Since a faster degradation process would have led to more uncertainty in the quantification of the released fraction, the experiments were carried out at a serum concentration of 10% assuring a good balance between the simulation of physiological conditions and the technical requirements of a time-resolved quantification (Jablonka et al., 2019; Jablonka et al., 2020b; Wallenwein et al., 2019).

3.3. Investigation of the drug release using the dispersion releaser technology

The *in vitro* release profiles of the Active Ingredient formulations NanoCore-7.4, Lipodox® NanoCore-6.4, and nCVTs-Dox were measured using the DR technology. The chemical stability and permeation of the drug are important reference experiments used in the

normalization of the release profile (Janas et al., 2017; Nothnagel and Wacker, 2018). The non-normalized release and drug permeation profiles are presented together in Figure 3 (left).

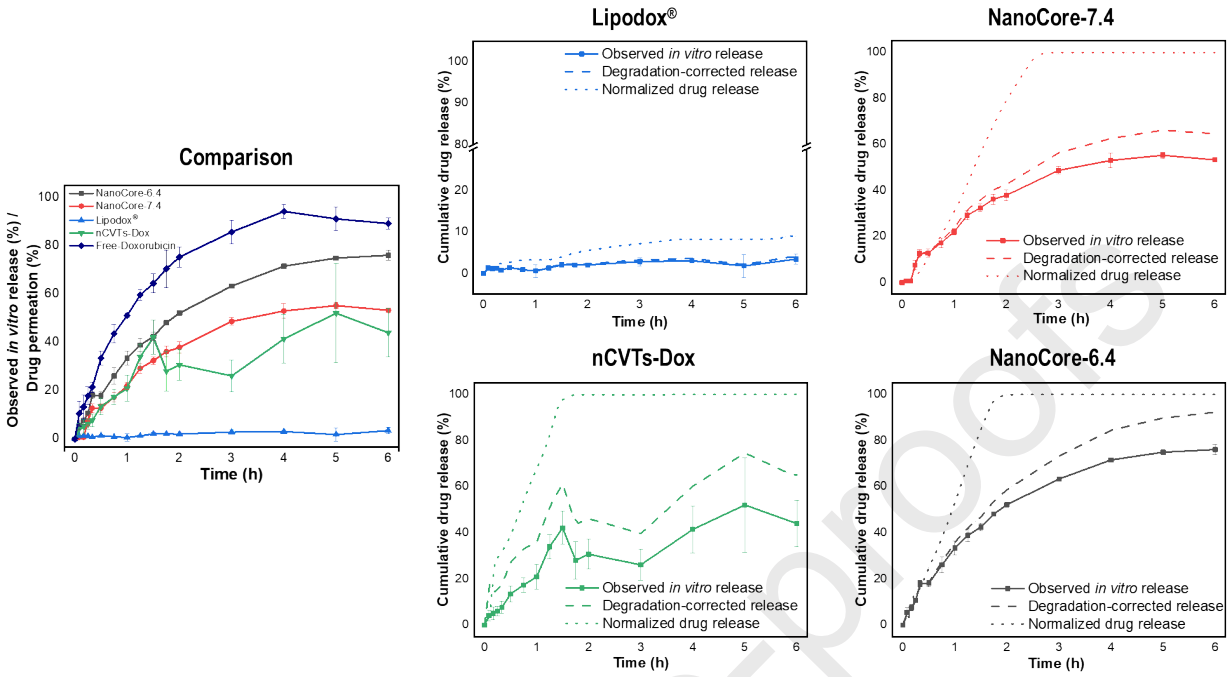

Figure 2. Non-normalized *in vitro* drug release profiles of Lipodox®, NanoCore-7.4, nCVTs-Dox, and NanoCore-6.4 and permeation profile of Active Ingredient observed in the DR (left). Comparison of the *in vitro* drug release profiles of each formulation with the degradation-corrected drug release profile, and the normalized drug release profile for Lipodox® (upper-middle), NanoCore-7.4 (upper-right), nCVTs-Dox (lower-middle), and NanoCore-6.4 (lower-right). Each of the measured release profiles is expressed as the average ± SD (n=3).

Expectedly, the most rapid release was observed for NanoCore-6.4 (Figure 3, lower-right), followed by the investigational drug product NanoCore-7.4 (Figure 3, upper-right). The *in vivo* behavior of these two formulation candidates has been investigated in much detail *in vitro* and *in vivo* (Kovshova et al., 2021). A total drug release of 76% was observed within 6 h for NanoCore-6.4, as compared to NanoCore-7.4 with a total release of 53% only.

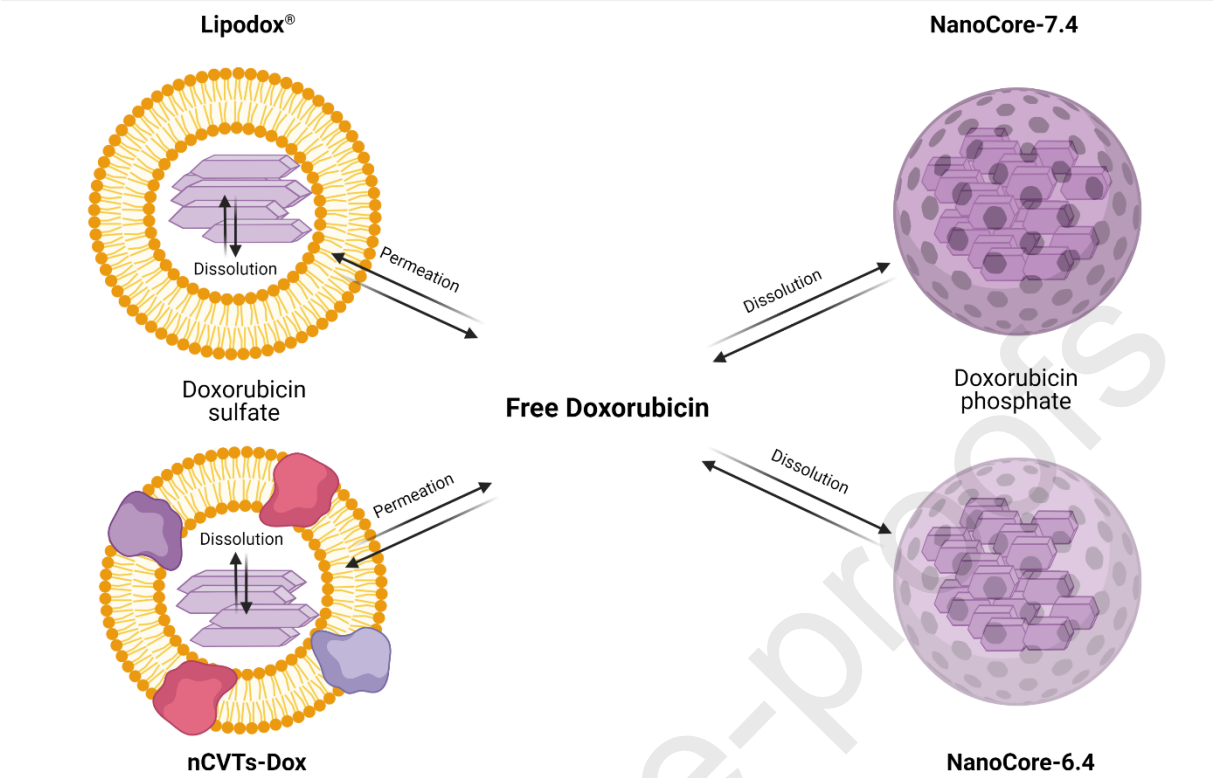

Figure 3. Illustration of the release mechanisms of Active Ingredient formulations. The release rate is limited by drug solubility in the microenvironment of the carrier. For liposomes, the permeation of the drug through the membrane plays a certain role as well.

The release of all four formulations is controlled by the solubility of Active Ingredient in the microenvironment of the carrier. NanoCore-6.4 and NanoCore-7.4 were synthesized at different pH values. At lower pH (6.4) the ionic equilibrium of the amphiphilic Active Ingredient molecule shifts toward the formation of cations with a protonated amino group. This leads to a lower affinity for the hydrophobic PLGA matrix (Fulop et al., 2013). At the higher pH (7.4), the formation of poorly soluble Active Ingredient phosphate enables slightly stronger matrix interactions (Maksimenko et al., 2019). Also, the pore structure of PLGA does not create an effective barrier prolonging the release phase.

Lipodox® exhibits the slowest release, reaching a total of 3.5% over 6 h (Figure 3, upper-middle). The formulation uses the remote loading process, resulting in the precipitation of Active Ingredient sulfate in the pegylated liposomes (Figure 4). The liposome provides a stable microenvironment, leading to sustained-release behavior (Barenholz, 2012; Lasic et al., 1995). This process has been applied in the synthesis of nCVTs-Dox as well (Figure 4).

The rate-limiting step in the release of all four drug formulations is the dissolution of Active Ingredient. Moderate aqueous solubility of the drug together with the degradation affect the concentration gradient. Still, permeation through the bilayer membranes of liposomes and nCVTs leads to different performances between polymeric nanoparticles and vesicles. This affects the IVIVC as well. While polymeric nanoparticles are insensitive to shear forces, the stirring rate can be assumed to have much a stronger impact on the release behavior of the vesicle system. Consequently, no extrapolations should be made between these two types of nanomedicines. Most surprisingly, the release of nCVTs-Dox was characterized by two distinct phases. After an initial increase, the concentration in the acceptor compartment lowered to approximately 20%, followed by the second release phase (Figure 3, middle-lower).

The delivery system was initially developed by Pastorin and co-workers to combine the advantages of liposomes with the superior targeting capabilities of extracellular vesicles. They are manufactured using an extrusion process (Goh et al., 2018) followed by remote loading of Active Ingredient. The presence of membrane proteins as well as the addition of the cell ghost suspension to the dehydrated film of phospholipids may lead to the formation of multiple fractions of vesicles. Even though this difference is observed *in vitro*, the corrected overall release rate was most comparable to the one of NanoCore-7.4. It is unlikely that these differences would have a major impact on plasma pharmacokinetics. However, nCVTs were found to exhibit an accumulation in the target tissue comparable to pegylated liposomes. Therefore, even with their rapid release, the formulation can be expected to have a strong pharmacological effect. However, further characterization would require a biodistribution study rather than an IVIVC based on the plasma concentration-time profile.

3.4. Estimation of the *in vivo* release

The PBNB model has been developed to systematically analyze the pharmacokinetics of nanocarrier formulations including a model-informed deconvolution of the total plasma concentration-time profile into the respective profiles of the free and the encapsulated fraction of the drug (Kovshova et al., 2021; Nagpal et al., 2020). A more detailed model validation based on preclinical and human clinical data was published previously (Kovshova et al., 2021; Nagpal et al., 2020).

The processes following the infusion of nanomedicines into the body can be explained as follows. After a short transit period in the blood vessels, the major fraction of the carrier-bound drug remains within the vascular system and is characterized by a small volume of distribution (1.928-2.756). The release of Active Ingredient in blood circulation represents the *in vivo* conversion of the encapsulated drug into the pharmacologically active form (Kovshova et al., 2021; Nagpal et al., 2020). It leads to a diffusion of the free drug into "deeper compartments". The free fraction has a 10-fold larger volume of distribution (26.908-27.22 L) and contributes to the clearance of the drug from blood circulation. by the distribution and recirculation rates identified from the pharmacokinetic profile of free Active Ingredient. Also, this parameter is unlikely to change for Active Ingredient which has a much lower affinity to phospholipids than observed for other compounds (Wallenwein et al., 2019).

A certain fraction of nanomedicines accumulates in organs or tissues. It is responsible for the altered biodistribution of the carrier-bound fraction. The recirculation of the drug into the vascular system was considered negligible. Two mechanisms could lead to such a recirculation effect, the diffusion of colloids from the peripheral tissues back into blood circulation or the intracellular release of Active Ingredient followed by diffusion of the free drug into the circulatory system.

The first mechanism, the diffusion of colloids back into blood circulation has been investigated *in vitro* and *in vivo*. For most nanomedicines, pharmacokinetics is accurately described by a one-compartment model and does not suggest the occurrence of recirculation (Kovshova et al., 2021; Nagpal et al., 2020). Also, blood partitioning of Lipodox® and NanoCore-7.4 has been investigated *in vitro* and led to a rapid equilibrium within a few minutes (Carter et al., 2019; Kovshova et al., 2021). Against this background, the first mechanism is unlikely to have a strong influence on plasma pharmacokinetics.

The second mechanism, the intracellular release of Active Ingredient, could lead to considerable recirculation as well. In this context, the low hemolysis in response to Lipodox® must be considered. It accounted for 2-5% of the total dose only (Carter et al., 2019). Also, a perfusion study in rats showed negligible Active Ingredient concentrations in the perfusate (Ballet et al., 1987). Both studies suggest a minor contribution of the intracellular release. However, even a more significant recirculation would hardly be reflected by the plasma concentration. A 10-fold larger volume of distribution of the free as compared to the

encapsulated drug reduces the impact dramatically.

To describe the accumulation of the carrier, the PBNB model calculates the carrier half-life ($t_{1/2}$). It is a measure of all accumulation and biodistribution processes including the binding of colloids to blood cells and depends on a wide variety of factors such as the particle size (Boerman et al., 1997) and the formation of a protein corona (Hadjidemetriou et al., 2016). For Lipodox®, an *in vivo* half-life of 89.79 h was identified while NanoCore-7.4 exhibits a much shorter half-life of 0.712 h in humans. So far, there are no *in vitro* methods to accurately predict the *in vivo* circulation time of nanomedicines. However, an accurate estimation was achieved for the short-circulating liposomal formulation Foslip using rat data (Jablonka et al., 2020b).

Noteworthy, a considerable fraction of the encapsulated drug will be absorbed after accumulation in organs or tissues without reappearing in the blood plasma. Following the current practices, this fraction cannot be further resolved based on phase-I clinical data alone. Therefore, the targeting capability (F_{target}) was introduced to the model. The drug formulation NanoCore-7.4 has a targeting capability of approximately 20%. Accordingly, about 80% of the injected dose of NanoCore-7.4 will follow the known distribution and elimination behavior of Active Ingredient, while only 20% may lead to a nanomaterial-related change in plasma pharmacokinetics (Mast et al., 2021). The parameter provides quantitative information on the impact of nanotechnology on the delivery system but also highlights the limitations of IVIVCs using plasma pharmacokinetics alone (Mast et al., 2021).

Due to the very rapid elimination of free Active Ingredient as well as the 10-fold larger volume of distribution, the drug release leads to a strong reduction in the blood plasma concentration as well. In this context, the PBNB model estimates the *in vivo* release using a highly flexible mathematical model allowing the simulation of immediate release and sustained release behavior (Nagpal et al., 2020).

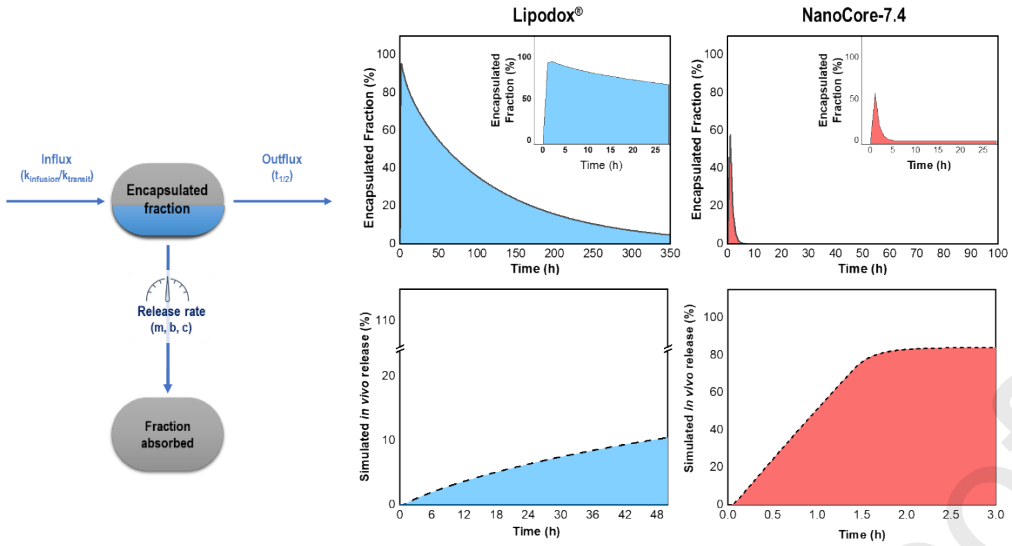

Figure 4. Illustration of the dose available for drug release in the *in vivo* situation (left) considering the continuous influx and outflux of the delivery system into and out of the blood plasma. The concentration levels depend on the infusion rate ($k_{infusion}$), the vascular transit rate (k_{trans}), and the elimination half-life of the nanocarrier ($t_{1/2}$). The encapsulated fraction (%) available in the blood plasma for Lipodox® (upper-middle) and NanoCore-7.4 (upper-right) as well as the simulated *in vivo* release (lower-middle and lower-right) corresponding to the *in vivo* release rate of Active Ingredient.

The complex interplay between the infusion of the drug, the circulation time, and the *in vivo* drug release is illustrated in Figure 5 (left). While the slow intravenous infusion of nanomedicines commonly follows zero-order influx kinetics, the accumulation in the periphery leads to a continuous outflux of the dose available for drug release. The encapsulated fractions (%) available in the blood plasma over time for Lipodox® and NanoCore-7.4 are presented in Figure 5 (upper-middle and upper-right), respectively. The *in vivo* release used to establish the IVIVC is presented in this Figure 5 (lower-middle and lower-right) as well.

In summary, the *in vivo* release of Active Ingredient from nanocarrier formulations is influenced by the influx (infusion and vascular transit), outflux (circulation time/ accumulation), and degradation of the compound. Therefore, it is not surprising that only a few examples of IVIVCs based on human clinical data of nanomedicines have been published (Díaz de León-Ortega et al., 2021) and, even more than 20 years after the approval of Active Ingredient®, liposomal formulations of Active Ingredient remained an unresolved challenge.

3.5. Establishing the *in vitro-in vivo* relationship

As outlined in the previous section, the *in vivo* release was extracted from the pharmacokinetic data reported for NanoCore-7.4 (Filon et al., 2017; Nagpal et al., 2020) and Lipodox® (Bhowmik et al., 2018; Nagpal et al., 2020). Due to the continuous accumulation of nanocarriers from the blood plasma and the relatively slow release observed for Lipodox®, the *in vivo* release of both formulations does not reach 100%. Even the *in vivo* release of the fast-releasing formulation NanoCore-7.4 reaches its plateau at approximately 80% with a fraction of approximately 20% accumulating in the body (reflected by the targeting capability, section 3.4).

Linearity was observed for the release phase before a plateau was reached. In both cases, the normalized *in vitro* release profile (Figure 3) and the *in vivo* release profile estimated by the PBNB model were used (Figure 5). Considering the coefficients of determination of 0.98648 (NanoCore-7.4) and 0.94107 (Lipodox®) as well as the significant differences in the release rate of the two formulations, the biorelevant *in vitro* release assay can be considered a valuable performance indicator in the estimation of human clinical data (Figure 6).

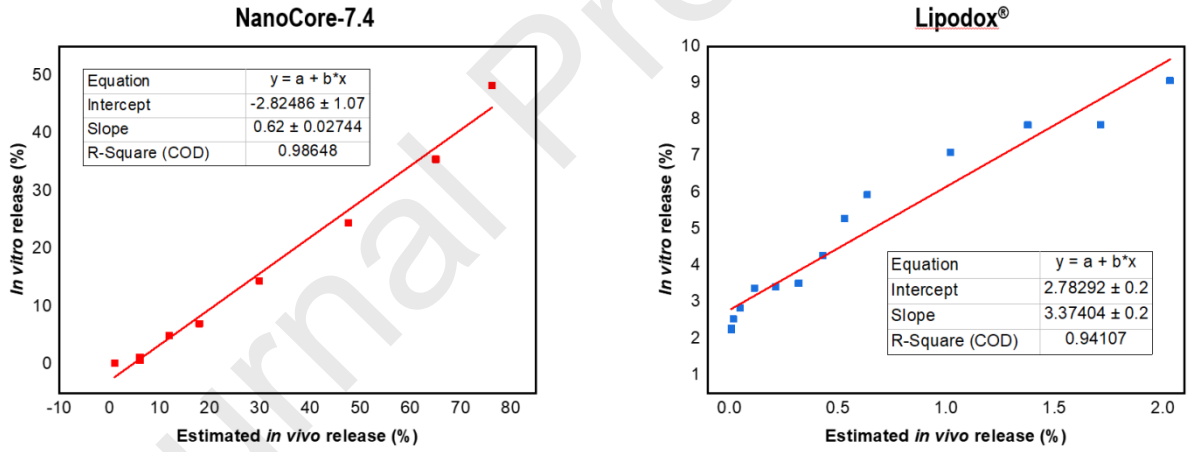

Figure 5. IVIVC of Lipodox® (right) and NanoCore-7.4 (left) based on human clinical data using the calculated *in vivo* release profile (Bhowmik et al., 2018; Nagpal et al., 2020; Panagi et al., 2001) and the normalized, degradation-corrected drug release profile. The *in vitro* and *in vivo* release profiles of Lipodox® and NanoCore-7.4 were fitted with the equation shown above.

A difference in slope indicates differences in the response of both formulation types to the *in vitro* conditions. In this context, the shear forces applied during the separation of nanomedicines from free Active Ingredient are the most likely explanation. While polymer nanoparticles exhibit a solid structure and are widely unaffected by continuous agitation, the permeability of the liposomal membrane is likely to change in response to the stirring rate. Therefore, all

estimations of pharmacokinetics were based on formulations most similar to the ones used for assay validation. This will be a subject of future investigations.

3.6. Estimation of human pharmacokinetics

To provide further proof for the validity of the simulations, human pharmacokinetics of Lipodox® and NanoCore-7.4 were calculated by using the *in vitro* release data. The *in vitro* release rate was extrapolated to cover the whole time of the study. A comparison with human clinical data is presented in Figure 7 (upper-left and upper-right). The plasma concentration of Lipodox® is slightly underestimated by the simulation but still within the standard deviations of the clinical trial (Figure 7, upper-left). This underestimation could be due to the V_{DC} estimated for this patient population or the *in vitro* release. Both parameters have a considerable influence. However, the release rate would affect the elimination of Active Ingredient from the blood plasma as well. Therefore, V_{DC} can be considered the most relevant error source. The prediction of NanoCore-7.4 is more accurate and reflects the *in vivo* performance of the particles.

In a second step, the *in vitro* release rates of NanoCore-6.4 and nCVTs-Dox were used in a prediction of human pharmacokinetics. Importantly, two parameters in this model simulation cannot be estimated based on the *in vitro* release, the vascular transit rate (k_{trans}) and the half-life of the carrier in blood circulation ($t_{1/2}$). While the vascular transit rate (k_{trans}) is a minor influence causing a small delay in the t_{max}, the carrier half-life ($t_{1/2}$) has a strong influence on the pharmacokinetic profile. Currently, even with the existing preclinical models in rodents or larger animals, a prediction of the circulation time is challenging. Therefore, we simulated optional scenarios for NanoCore-6.4 and nCVTs based on their physicochemical characteristics and surface properties. These simulations require careful interpretation and are widely based on the assumption that the physicochemical characteristics and preclinical studies in rodents will reflect the clinical reality. Also, to exclude a change in the physicochemical characteristics, the *in vitro* stability of the novel formulation candidates NanoCore-6.4 and nCVTs were investigated in presence of serum proteins. All formulations were stable over 24 h (**supplementary materials, S4**).

The carrier half-lives observed in the two clinical trials for NanoCore-7.4 (Filon et al., 2017) and Lipodox® (Bhowmik et al., 2018) span a wide range from 0.712-89.79 h. The first simulation predicting the pharmacokinetics of NanoCore-6.4 uses the whole range (Figure 7,

lower-right/yellow lines). The simulation provides the 'best possible scenario' and highlights the drug release as a limiting factor in pharmacokinetics. Even when simulating much longer half-lives, the drug is completely eliminated from the blood plasma within 100 . For this formulation, much longer half-lives as compared to NanoCore-7.4 seem unlikely. The non-pegylated PLGA nanoparticles are rapidly recognized by the cells of the reticuloendothelial system (RES) and eliminated from blood circulation (Kovshova et al., 2021). Therefore, the second simulation was carried out assuming the elimination rate of NanoCore-6.4 to be very similar to NanoCore-7.4, modeling variations in the half-life of ± 20% (0.57-0.85 h). The outcome of this simulation is presented in Figure 7 (lower-right/black lines). It provides a more realistic estimate of the *in vivo* performance. This is further confirmed by the pharmacokinetic studies in rats showing a very similar pharmacokinetic behavior for NanoCore-6.4 and NanoCore-7.4.

nCVTs-Dox were manufactured by the extrusion of cells combined with phospholipids and cholesterol. The vesicle structure is most comparable to non-pegylated liposomes. However, the influence of cellular phospholipids, as well as the decoration with surface proteins, may have a strong impact on the circulation time. In the first simulation, we calculated circulation times in a range of 0.712-89.79 h (Figure 7 lower-left/light green lines). With regards to the phospholipids added during synthesis, the composition was most comparable to the established drug products Foslip® and Myocet® with half-lives ranging from 23.32 h (Foslip®) to 14.34 h (Myocet®). This range was used for the second simulation (Figure 7, lower-left, yellow lines). The third simulation considered the diameter of the vesicles. nCVTs-Dox had a diameter of 194 ± 12.4 nm. For comparison, the liposomal drug product Myocet® has an average vesicle diameter of 190 nm. Therefore, we simulated circulation times comparable to Myocet® including a variation of ± 20% in the same range (Figure 7, lower-left/dark green).
Importantly, all simulations carried out for nCVTs come with high uncertainty.

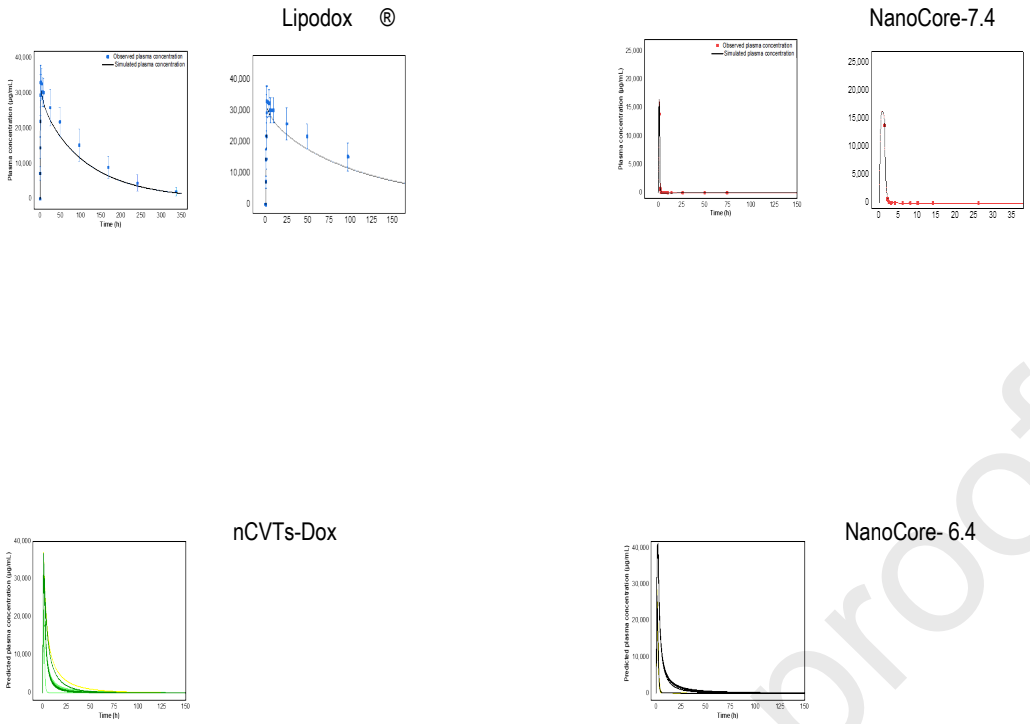

Figure 6. Comparison of observed plasma concentration and simulated in vivo pharmacokinetics of Lipodox® (upper left) and NanoCore-7.4 (upper right) using the PBNB model. Simulated in vivo pharmacokinetics of nCVTs-Dox (lower left) and NanoCore-6.4 (lower-right). Simulated variations in the carrier half-life of nCVTs include ranges of 0.712-89.79 h (light green lines), 14.34-23.32 h (yellow lines), and 11.47-17.21 h (green lines). For NanoCore-6.4 ranges of 0.712-89.79 h (black lines) and 0.57-0.85 h (yellow lines) were simulated.

Still, our estimations indicate that the *in vivo* release limits the overall exposure with Active Ingredient to the first 100 h. Therefore, in addition to exploring the circulation time of the carrier, the remote loading procedure must be further optimized before the drug delivery system can be evaluated in preclinical or clinical studies. This is reflected by the targeting capability as well. Because of the rapid release, the targeting capability of nCVTs reaches a maximum of approximately 15%. For comparison, Lipodox® reaches a targeting capability of approximately 95% (Nagpal et al., 2020).

4. Conclusion

In the present approach, we established an IVIVC using the *in vitro* release profiles measured with the DR technology. Applying the assay in the estimation of *in vivo* performances is sustained by the coefficients of determination of the IVIVCs obtained for Lipodox® and NanoCore-7.4. A hybrid physiologically-based biopharmaceutics (PBB) model was used to calculate the *in vivo* release. The circulation half-life of the carrier remains an important challenge in the prediction of human pharmacokinetics. Still, the *in vivo* performances of the novel formulation candidates, NanoCore-6.4 and nCVTs-Dox, were predicted based on structural similarities with the nanocarriers. Such material-based predictions come with a high uncertainty but may reduce the risk of failure during the phase-I clinical trials. They guide formulation development in the optimization of critical quality attributes and represent a cornerstone in the development of nanopharmaceuticals. Further, our work highlights the importance of computational methods and modeling approaches in the evaluation and interpretation of clinical data obtained with nanomedicines.

5. Acknowledgments

The authors acknowledge the National University of Singapore (grant no. R-148-000-282-133 and R-148-000-297-114) and the Russian Foundation of Basic Research (project no. 20-015-00276) for financial support. Also, we would like to thank Lixoft (Antony, France) for supporting us with an academic license of Monolix Suite 2020, Corbion for providing us with Pura Sorb, and Sun Pharmaceutical Industries Ltd for kindly providing us with Lipodox®.

6. References

Alibolandi, M., Abnous, K., Mohammadi, M., Hadizadeh, F., Sadeghi, F., Taghavi, S., Jaafari, M.R., Ramezani, M., 2017. Extensive preclinical investigation of polymersomal formulation of Active Ingredient versus Active Ingredient-mimic formulation. J Control Release 264, 228-236.

Ballet, F., Vrignaud, P., Robert, J., Rey, C., Poupon, R., 1987. Hepatic extraction, metabolism and biliary excretion of Active Ingredient in the isolated perfused rat liver. Cancer Chemother Pharmacol 19, 240-245.

Barenholz, Y., 2012. Active Ingredient(R)--the first FDA-approved nano-drug: lessons learned. J Control Release 160, 117-134.

Bhowmik, S., Bhowmick, S., Maiti, K., Chakra, A., Shahi, P., Jain, D., Rajamannar, T., 2018. Two multicenter Phase I randomized trials to compare the bioequivalence and safety of a generic Active Ingredient hydrochloride liposome injection with Active Ingredient® or Caelyx® in advanced ovarian cancer. Cancer Chemotherapy and Pharmacology 82, 521-532.

Boerman, O.C., Oyen, W.J., van Bloois, L., Koenders, E.B., van der Meer, J.W., Corstens, F.H., Storm, G., 1997. Optimization of Active Ingredient-99m-labeled PEG liposomes to image focal infection: effects of particle size and circulation time. J Nucl Med 38, 489-493.

Carter, K.A., Luo, D., Geng, J., Stern, S.T., Lovell, J.F., 2019. Blood Interactions, Pharmacokinetics, and Depth-Dependent Ablation of Rat Mammary Tumors with Photoactivatable, Liposomal Active Ingredient. Molecular Cancer Therapeutics 18, 592-601.

Cheng, C., Wu, P.-C., Lee, H.-Y., Hsu, K.-Y., 2014. Development and validation of an in vitro–in vivo correlation (IVIVC) model for Active Ingredient hydrochloride extended-release matrix formulations. journal of food and drug analysis 22, 257-263.

Díaz de León-Ortega, R., D'Arcy, D.M., Lamprou, D.A., Xue, W.F., Fotaki, N., 2021. In vitro in vivo relations for the parenteral liposomal formulation of Active Ingredient B: A biorelevant and clinically relevant approach. Eur J Pharm Biopharm 159, 188-197.

El-Kareh, A.W., Secomb, T.W., 2000. A mathematical model for comparison of bolus injection, continuous infusion, and liposomal delivery of Active Ingredient to tumor cells. Neoplasia 2, 325-338.

Fecioru, E., Klein, M., Kramer, J., Wacker, M.G., 2019. In Vitro Performance Testing of Nanoparticulate Drug Products for Parenteral Administration. Dissolution Technologies 26, 28+.

Feczko, T., Piiper, A., Ansar, S., Blixt, F.W., Ashtikar, M., Schiffmann, S., Ulshofer, T., Parnham, M.J., Harel, Y., Israel, L.L., Lellouche, J.P., Wacker, M.G., 2019. Stimulating brain recovery after stroke using theranostic albumin nanocarriers loaded with nerve growth factor in combination therapy. J Control Release 293, 63-72.

Filon, O., Krivorotko, P., Kobyakov, G., Razjivina, V., Maximenko, O., Gelperina, S., Kreuter, J., 2017. A phase I study of safety and pharmacokinetics of NanoBB-1-Dox in patients with advanced solid tumors. Journal of Clinical Oncology 35, e13537-e13537.

Fulop, Z., Gref, R., Loftsson, T., 2013. A permeation method for detection of self-aggregation of Active Ingredient in aqueous environment. Int J Pharm 454, 559-561.

Goh, W.J., Zou, S., Czarny, B., Pastorin, G., 2018. nCVTs: a hybrid smart tumour targeting platform. Nanoscale 10, 6812-6819.

Hadjidemetriou, M., Al-Ahmady, Z., Kostarelos, K., 2016. Time-evolution of in vivo protein corona onto blood-circulating PEGylated liposomal Active Ingredient (Active Ingredient) nanoparticles. Nanoscale 8, 6948-6957.

Hinderliter, P., Saghir, S.A., 2014. Pharmacokinetics, in: Wexler, P. (Ed.), Encyclopedia of Toxicology (Third Edition). Academic Press, Oxford, pp. 849-855.

Jablonka, L., Ashtikar, M., Fiona Gao, G., Thurn, M., Modh, H., Wang, J.W., Preuss, A., Scheglmann, D., Albrecht, V., Roder, B., Wacker, M.G., 2020a. Predicting human pharmacokinetics of liposomal temoporfin using a hybrid in silico model. Eur J Pharm Biopharm 149, 121-134.

Jablonka, L., Ashtikar, M., Gao, G., Jung, F., Thurn, M., Preuß, A., Scheglmann, D., Albrecht, V., Röder, B., Wacker, M.G., 2019. Advanced in silico modeling explains pharmacokinetics and biodistribution of temoporfin nanocrystals in humans. J Control Release 308, 57-70.

Jablonka, L., Ashtikar, M., Gao, G.F., Thurn, M., Modh, H., Wang, J.W., Preuss, A., Scheglmann, D., Albrecht, V., Roder, B., Wacker, M.G., 2020b. Predicting human pharmacokinetics of liposomal temoporfin using a hybrid in silico model. Eur J Pharm Biopharm 149, 121-134.

Janas, C., Mast, M.P., Kirsamer, L., Angioni, C., Gao, F., Mantele, W., Dressman, J., Wacker, M.G., 2017. The dispersion releaser technology is an effective method for testing drug release from nanosized drug carriers. Eur J Pharm Biopharm 115, 73-83.

Kovshova, T., Osipova, N., Alekseeva, A., Malinovskaya, J., Belov, A., Budko, A., Pavlova, G., Maksimenko, O., Nagpal, S., Braner, S., Modh, H., Balabanyan, V., Wacker, M.G.,

Gelperina, S., 2021. Exploring the Interplay between Drug Release and Targeting of Lipid-Like Polymer Nanoparticles Loaded with Active Ingredient. 26, 831.
Lasic, D.D., Ceh, B., Stuart, M.C., Guo, L., Frederik, P.M., Barenholz, Y., 1995. Transmembrane gradient driven phase transitions within vesicles: lessons for drug delivery. Biochim Biophys Acta 1239, 145-156.
Laubrock, N., Hempel, G., Schulze-Westhoff, P., Würthwein, G., Flege, S., Boos, J., 2000. The stability of Active Ingredient and ldarubicin in plasma and whole blood. Chromatographia 52, 9-13. Maksimenko, O., Malinovskaya, J., Shipulo, E., Osipova, N., Razzhivina, V., Arantseva, D., Yarovaya, O., Mostovaya, U., Khalansky, A., Fedoseeva, V., Alekseeva, A., Vanchugova, L., Gorshkova, M., Kovalenko, E., Balabanyan, V., Melnikov, P., Baklaushev, V., Chekhonin, V., Kreuter, J., Gelperina, S., 2019. Active Ingredient-loaded PLGA nanoparticles for the chemotherapy of glioblastoma: Towards the pharmaceutical development. Int J Pharm 572, 118733.
Mast, M.P., Modh, H., Champanhac, C., Wang, J.W., Storm, G., Kramer, J., Mailander, V., Pastorin, G., Wacker, M.G., 2021. Nanomedicine at the crossroads - a quick guide for ivivc. Adv Drug Deliv Rev, 113829.
Nagpal, S., Braner, S., Modh, H., Tan, A.X.X., Mast, M.P., Chichakly, K., Albrecht, V., Wacker, M.G., 2020. A physiologically-based nanocarrier biopharmaceutics model to reverse-engineer the in vivo drug release. Eur J Pharm Biopharm 153, 257-272.
Nothnagel, L., Wacker, M.G., 2018. How to measure release from nanosized carriers? Eur J Pharm Sci 120, 199-211.
Pereverzeva, E., Treschalin, I., Treschalin, M., Arantseva, D., Ermolenko, Y., Kumskova, N., Maksimenko, O., Balabanyan, V., Kreuter, J., Gelperina, S., 2019. Toxicological study of Active Ingredient-loaded PLGA nanoparticles for the treatment of glioblastoma. Int J Pharm 554, 161-178.
Ritschel, W., Kearns, G., 2009. Chapter 2. The LADMER System: Liberation, Absorption, Distribution, Metabolism, Elimination, and Response, Handbook of Basic Pharmacokinetics… Including Clinical Applications, 7th Edition.
Shen, J., Burgess, D.J., 2015. In vitro-in vivo correlation for complex non-oral drug products: Where do we stand? J Control Release 219, 644-651.
Storn, R., Price, K., 1997. Differential Evolution – A Simple and Efficient Heuristic for global Optimization over Continuous Spaces. J Global Optim 11, 341-359.
Villa Nova, M., Janas, C., Schmidt, M., Ulshoefer, T., Grafe, S., Schiffmann, S., de Bruin, N., Wiehe, A., Albrecht, V., Parnham, M.J., Luciano Bruschi, M., Wacker, M.G., 2015. Nanocarriers for photodynamic therapy-rational formulation design and medium-scale manufacture. Int J Pharm 491, 250-260.
Wallenwein, C.M., Nova, M.V., Janas, C., Jablonka, L., Gao, G.F., Thurn, M., Albrecht, V., Wiehe, A., Wacker, M.G., 2019. A dialysis-based in vitro drug release assay to study dynamics of the drug-protein transfer of temoporfin liposomes. Eur J Pharm Biopharm 143, 44-50.
Xie, L., Beyer, S., Vogel, V., Wacker, M.G., Mantele, W., 2015. Assessing the drug release from nanoparticles: Overcoming the shortcomings of dialysis by using novel optical techniques and a mathematical model. Int J Pharm 488, 108-119.
Yong, T., Wang, D., Li, X., Yan, Y., Hu, J., Gan, L., Yang, X., 2020. Extracellular vesicles for tumor targeting delivery based on five features principle. J Control Release 322, 555-565.
Zhang, E., Zhukova, V., Semyonkin, A., Osipova, N., Malinovskaya, Y., Maksimenko, O., Chernikov, V., Sokolov, M., Grigartzik, L., Sabel, B.A., Gelperina, S., Henrich-Noack, P., 2020. Release kinetics of fluorescent dyes from PLGA nanoparticles in retinal blood vessels: In vivo monitoring and ex vivo localization. Eur J Pharm Biopharm 150, 131-142.

Harshvardhan Modh: conceptualization, investigation, data curation, writing - original draft; Daniel Juncheng Fang: validation; Yi Hsuan Ou: investigation, data curation; Jia Ning Nicolette Yau: investigation, data curation; Tatyana Kovshova: investigation, data curation; Shakti Nagpal: formal analysis, writing – editing & review; Julian Knoll: data curation, formal analysis, writing – editing & review; Chantal M. Wallenwein: writing – editing & review, visualization; Kuntal Maiti: resources; Subdhas Bhowmick: resources; Svetlana Gelperina: project administration, funding acquisition, supervision, writing – editing & review; Giorgia Pastorin: project administration, funding acquisition, supervision, writing – editing & review; Matthias G. Wacker: conceptualization, project administration, funding acquisition, supervision, writing – editing & review, visualization.

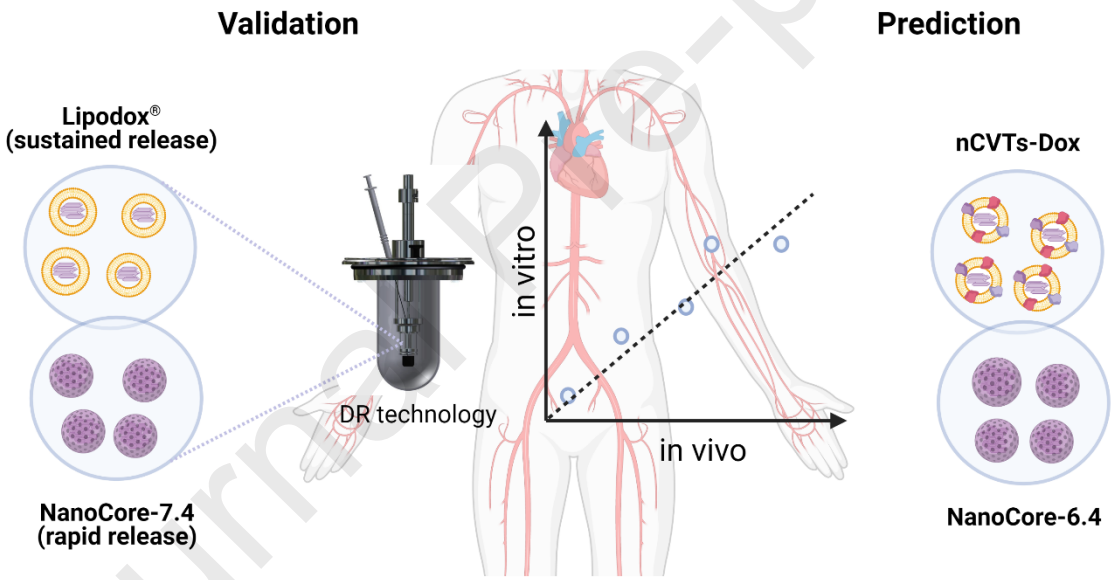

Declaration of interests

☒ The authors declare that they have no known competing financial interests or personal relationships that could have appeared to influence the work reported in this paper.

☐The authors declare the following financial interests/personal relationships which may be considered as potential competing interests: